Turbulent clustering of stagnation points and inertial particles

By L. CHEN[1], S. GOTO[2] AND J. C. VASSILICOS[1,3]

[1]Department of Aeronautics, Imperial College London, SW7 2AZ, UK

[2]Department of Mechanical Engineering and Science, Kyoto University, 606-8501, Japan

[3]Institute for Mathematical Sciences, Imperial College London, SW7 2AZ, UK

In high-Reynolds-number two-dimensional turbulence with a $-5/3$ power-law energy spectrum, the clustering of inertial particles reflects the clustering of acceleration stagnation points for all particle relaxation times smaller than the integral time scale T of the turbulence. Acceleration stagnation points and small inertial particles on these points are swept together by large-scale motions. In synthetic turbulence where there is no sweeping and acceleration stagnation points do not cluster, inertial particles do nevertheless cluster as a result of the repelling action of persistent velocity stagnation-point clusters. This repelling action has a negligible effect on the clustering of inertial particles in the presence of acceleration stagnation points clustering.

1. Introduction

In many environmental, geophysical and industrial processes, inertial particles or droplets interact with turbulent flows to generate complex clustering patterns and concentration fluctuations which can, via an agglomeration process, lead to enhanced precipitation in clouds and powders in the chemical and pharmaceutical industries. Fluctuations in particle concentrations and clusters are also responsible for large variations in the efficiency of various industrial processes and characterize air pollution in cities and elsewhere.

Here, we consider small aerosols or droplets (e.g. cloud droplets) in gases subjected to linear Stokes drag. Gravity is ignored because the central concern in this paper is the clustering of identical inertial particles. The particles/droplets are assumed spherical with a radius a smaller than the smallest length scale of the turbulence, a density much larger than that of the ambient fluid and a particle Reynolds number much smaller than 1. The equation of motion of such particles is approximated well by (see Maxey & Riley 1983)

$$\frac{\mathrm{d}}{\mathrm{d}t}\boldsymbol{v} = \frac{1}{\tau_p}[\boldsymbol{u}(\boldsymbol{x}_p, t) - \boldsymbol{v}(t)] \tag{1}$$

where $\boldsymbol{v}(t)$ is the velocity of the particle/droplet at its position $\boldsymbol{x}_p(t)$ at time t, $\boldsymbol{u}(\boldsymbol{x}, t)$ the fluid velocity field, $\tau_p = 2\rho_p a^2/(9\mu)$ the particle relaxation time, ρ_p the particle's mass density and μ the surrounding fluid's dynamic viscosity. We also assume that the particles do not significantly affect the fluid turbulence and that they are dilute enough not to interfere with each other.

Recent results on inertial particle clustering obtained with two-dimensional and three-dimensional direct numerical simulation (DNS) have been reported by Boffetta,

De Lillo & Gamba (2004) and Collins & Keswani (2004). In the present paper, the emphasis is on high-Reynolds-number turbulence with well-defined power-law energy spectra, which is why we concentrate on two-dimensional turbulence. However we attempt to interpret particle clustering in specific stagnation-point terms which may also be valid in three-dimensional turbulence, though we leave three-dimensional turbulence for future study. We simulate two-dimensional inverse-energy-cascading statistically homogeneous turbulent velocity fields $u(x, t)$ by DNS following the method detailed in Goto & Vassilicos (2004; referred to as GV hereafter) which gives a well-defined $-5/3$ power-law energy spectrum. We also simulate two-dimensional statistically homogeneous turbulent-like velocity fields with a $-5/3$ power-law energy spectrum by kinematic simulation (KS) (Fung & Vassilicos 1998; referred to as FV hereafter). Instead of Reynolds numbers, we will be referring to outer- to inner-length scale ratios L/η where L is the integral length scale in our DNS but the length scale corresponding to the smallest wavenumber in our KS and η is the small-scale forcing length scale in our DNS but the length scale corresponding to the small-scale end of the power-law energy spectrum in our KS. The corresponding outer- to inner-time scale ratio is T/τ_η. Inertial particles are characterized by their Stokes number $St = \tau_p/\tau_\eta$. In all our simulations, $St \leqslant T/\tau_\eta$.

2. Brief details of simulations

Full accounts of our simulations can be found in GV for the two-dimensional DNS and in FV and §6 for the two-dimensional KS. Here we just state that we are experimenting with two-dimensional DNS turbulence that has a well-defined $k^{-5/3}$ energy spectrum over a broad range of scales with $L/\eta = 30$ ($T/\tau_\eta = 25$) by using 4096^2 grid points (run D in GV); and that our KS velocity fields have power-law energy spectra $E(k) \sim k^{-5/3}$ in the range of wavenumbers $2\pi/L$ to $2\pi/\eta$ and no energy outside this range. The time dependence of the KS velocity fields is determined via the frequency $\omega(k) = \lambda\sqrt{k^3 E(k)}$ where λ is a dimensionless parameter controlling the intensity of the time dependence of the fluid velocity. $L/\eta = 10^3$ (except when a dependence on L/η is sought) and $T/\tau_\eta = O(100)$.

The one DNS check of a L/η scaling in §4 is made with the following two-dimensional DNS velocity fields from GV: run A, 512^2, $L/\eta = 6.3$ and $T/\tau_\eta = 10$; run B, 1024^2, $L/\eta = 10$ and $T/\tau_\eta = 13$; run C, 2048^2, $L/\eta = 19$ and $T/\tau_\eta = 19$; and run D above.

3. Clustering of inertial particles

Our DNS visualizations show that inertial-particle position fields starting from initial uniformity develop well-defined near-empty spaces as time progresses (see figure 1). It is striking that the locations of these near-empty spaces at given integration times are the same for all Stokes numbers. What differs from one Stokes number to another is the size of these regions, the average size of which increases with increasing Stokes number (see Goto & Vassilicos 2006 for quantitative details and also Falkovich, Fouxon & Stepanov 2003). All these observations are valid for any integration time that is long enough in comparison to τ_p.

In approximate agreement with the three-dimensional DNS of Collins & Keswani (2004), we find $\langle|\boldsymbol{\omega}|^2\rangle_p/\langle|\mathbf{s}|^2\rangle_p \approx 1$ for $0.1 < St < 1$ in our two-dimensional DNS ($\boldsymbol{\omega}$ and $\mathbf{s}$ are the vorticity and the strain-rate tensor respectively and the average operation $\langle\ldots\rangle_p$ is taken over Lagrangian points on all particle trajectories at a given
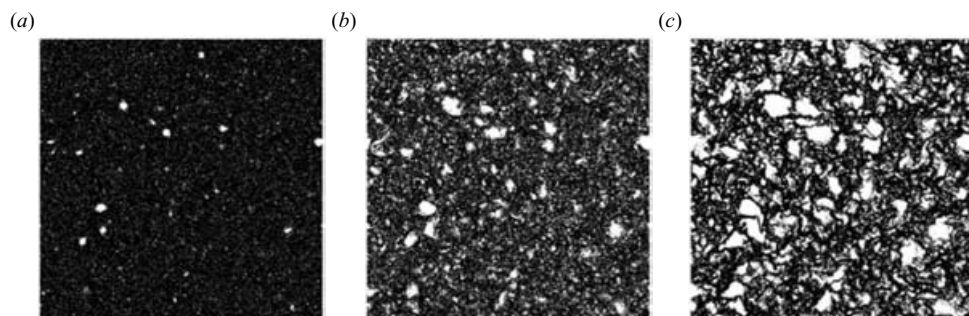
FIGURE 1. Particle distributions in two-dimensional DNS turbulence for three different Stokes numbers; (*a*) $St = 0.1$, (*b*) $St = 0.8$ and (*c*) $St = 6.4$. The entire simulation domain (about $27L$ in size) is shown and each black dot represents an inertial particle.

time). For $St > 1$ we find $\langle|\boldsymbol{\omega}|^2\rangle_p/\langle|\mathbf{s}|^2\rangle_p \approx 2$. This value 2 might suggest spatial uniformity because, in statistically homogeneous turbulence, $\langle|\boldsymbol{\omega}|^2\rangle/\langle|\mathbf{s}|^2\rangle = 2$ where the average operation $\langle\ldots\rangle$ is taken over all space. However, such uniformity is not observed in our visualizations of spatial distributions of inertial particles (see figure 1*c*). Furthermore, in the case of figure 1(*c*), where $St = 6.4$, as in all cases with large enough values of St, $\langle|\boldsymbol{\omega}|^2\rangle_p = \langle|\boldsymbol{\omega}|^2\rangle$. Hence, the generation of near-empty spaces cannot be fully understood in terms of inertial particles escaping high-vorticity regions because near-empty spaces also appear when $St > 1$.

4. Acceleration stagnation points

Nevertheless, we do expect the clustering of inertial particles to be determined by some sort of eddying action even though the statistics of vorticity and strain-rate tensor fail to fully correlate with this clustering. 'Eddies' are an undefined concept, so here we focus attention on the stagnation points of the fluid velocity field $\boldsymbol{u}(\boldsymbol{x}, t)$ and of the fluid acceleration field $\boldsymbol{a}(\boldsymbol{x}, t)$. In this, we follow the approach of FV, Davila & Vassilicos (2003), GV, Goto *et al.* (2005) and Osborne *et al.* (2006) who showed that velocity stagnation points have an impact on turbulent pair diffusion by virtue of the strong curvature of streamlines in their vicinity as they turn out to be persistent enough in time in a statistical sense which they define. Here we discuss how the statistics of stagnation points (both zero-velocity and zero-acceleration ones) can also have an impact on particle clustering.

Acceleration stagnation points, i.e. zero-acceleration points, might be thought of as points at the centre of vortices or between them. In figure 2 we visualize the spatial distribution of zero-acceleration points and the spatial distribution of inertial particles (the zero-acceleration points and the zero-velocity points in §7 are found using a tested Newton–Raphson iterative method as in GV). The remarkable spatial correlation which exists between these two spatial distributions is striking. The initial distribution of inertial particles was set uniform in space, and the snapshots in figure 2 have been obtained at a time long enough compared to τ_p. In fact, any such long time presents the remarkable spatial correlation shown in figure 2. As evidenced by results such as those in figure 1, the near-empty spaces characterizing the clustering of inertial particles are at the same places for different Stokes numbers but with different sizes. Hence, the clustering of zero-acceleration points determines the clustering of inertial particles but the Stokes number determines the characteristic size of the largest near-empty regions generated by the clustering.
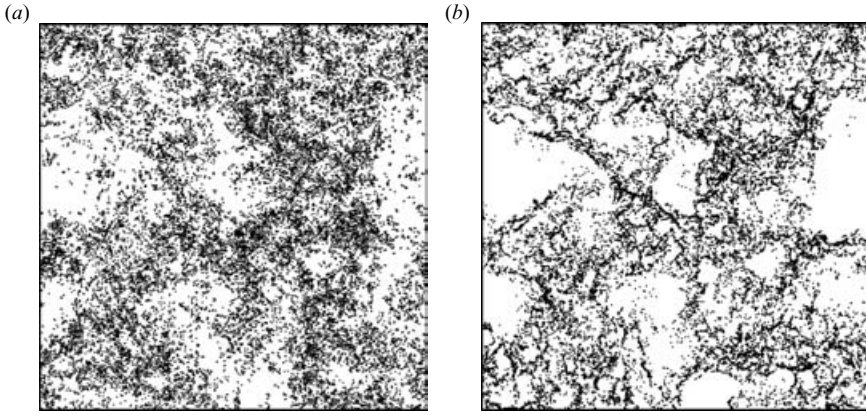
(*a*) (*b*)

FIGURE 2. Distribution of (*a*) inertial particles ($St = 1.9$) (represented by black dots) and (*b*) zero acceleration points (represented by black dots). Two-dimensional DNS. Box size is about $4L$.

We now present a property which is particular to the acceleration field and which, as we argue in the remainder of this paper, is closely related to the clustering of zero-acceleration points and of inertial particles. Generalizing the approach of Goto *et al.* (2005) and Osborne *et al.* (2006) to zero-acceleration points, we define these points $s_a(t)$ by $a(s_a(t), t) = 0$, their velocity by $V_a \equiv (d/dt)s_a(t)$ and write

$$\frac{D}{Dt}a + (V_a - u)\cdot\nabla a = 0 \tag{2}$$

at these points, where D/Dt is the Lagrangian time derivative following fluid elements and u is the fluid velocity at $s_a(t)$ at time t. Assuming that $(V_a - u)$ and ∇a are statistically uncorrelated, we deduce that

$$\langle|V_a - u|^2\rangle^{1/2} \sim \left\langle\left|\frac{D}{Dt}a\right|^2\right\rangle^{1/2}\tau_\eta^2 \tag{3}$$

where we reasonably assume Kolmogorov scaling for acceleration gradients. Such scaling can be applied to $(D/Dt)a$ and implies that $\langle|(D/Dt)a|^2\rangle^{1/2} \sim (u'^3/L^2)(L/\eta)$, where u' is the r.m.s. turbulent fluid velocity, which in turn implies

$$\langle(V_a - u)^2\rangle^{1/2} \sim u'(L/\eta)^{-1/3}. \tag{4}$$

The important consequence is that $\langle(V_a - u)^2\rangle^{1/2}/u' \to 0$ as $L/\eta \to \infty$, meaning that in the limit of high Reynolds numbers, zero-acceleration points move with their local fluid velocity u. This conclusion is valid for any constant-acceleration point, not only zero-acceleration points, and can be seen as a quantitative formulation of the Tennekes sweeping hypothesis which states that energy-containing turbulent eddies advect small-sale dissipative turbulent eddies (Tennekes 1975). The scaling relation (4) is validated by our two-dimensional DNS (see figure 3; V_a in the left-hand side of (4) was calculated by inverting (2) at zero-acceleration points).

For $St \leqslant 0.3$ (see Falkovich & Pumir 2004), $v \approx u - \tau_p a$ and $(d/dt)v = (u - v)/\tau_p$ so that an inertial particle at a zero-acceleration point moves, on average, *with* this zero-acceleration point when $L/\eta \gg 1$ (see equation (4)) because they both move, statistically, approximately with the same velocity u. Furthermore, the acceleration $(d/dt)v$ of an inertial particle at a zero-acceleration point is zero, thus reducing the particle's ability to escape from the zero-acceleration point. Instead, inertial particles
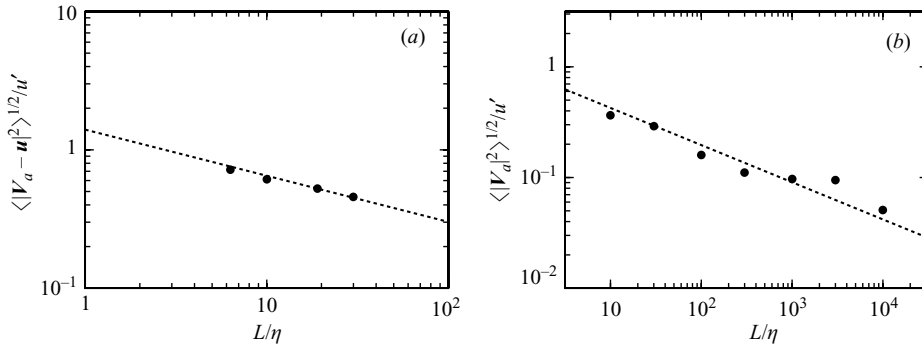
FIGURE 3. (*a*) R.m.s. value of $(V_a - u)/u'$ as function of L/η in DNS. (*b*) R.m.s. value of V_a/u' as function of L/η in KS with $\lambda = 0.5$. Dotted lines indicate $-1/3$ power law.

at points with high acceleration values readily move away from such points. Zero-acceleration points are therefore 'sticky' for inertial particles, whereas high-acceleration points are repellent (in the sense that particles at zero-acceleration points remain in their vicinity (while moving with them) for much longer than particles remain in the vicinity of a given high-acceleration point). This conclusion has been reached for small Stokes numbers but computational results such as those of figures 1 and 2 suggest that it might be valid for a wide range of Stokes numbers all the way up to T/τ_η, and in fact for an increasing portion of space as Stokes number increases. Indeed, at points where the local time scales of the fluid flow are very much larger than τ_p, the particle may be considered as a fluid element, so that $v \approx u$ irrespective of a. The different values of v for different local values of a can only occur where τ_p is not so much smaller than the fluid flow's local time scales. The larger the Stokes number, the larger the portion of space where fluid acceleration differences may have an impact on particle velocities.

The previous paragraph's argument (further expanded and clarified in Goto & Vassilicos 2006) may go some way in explaining why the spatial clusterings of acceleration stagnation points and of inertial particles are so well correlated.

5. Pair correlation functions

To measure clustering we use pair correlation functions which are simply related to the radial distribution function (Sundaram & Collins 1997) and the clustering index which is popular in analyses of observational data of atmospheric clouds (Kostinski & Jameson 2000; Kostinski & Shaw 2001; Shaw, Kostinski & Larsen 2002). The use of the pair correlation function is based on the correlation fluctuation theorem (Landau & Lifshitz 1980). This theorem states that if a grid of spacing r is superimposed on a spatial distribution of points, then the average pair correlation function $\overline{m}(r) \equiv (1/r) \int_0^r m(r') \, dr'$ is given by

$$\overline{m}(r) = \frac{\langle (\delta N)^2 \rangle_r}{\langle N \rangle_r^2} - \frac{1}{\langle N \rangle_r} \qquad (5)$$

where N is the number of points in each box, $\langle N \rangle_r$ the average number of points over all boxes and $\langle (\delta N)^2 \rangle_r = \langle (N - \langle N \rangle)^2 \rangle_r$ (where the average is taken over all boxes of size r). To educe average pair correlation functions of spatial distributions of inertial particles, zero-velocity points and zero-acceleration points from our turbulence
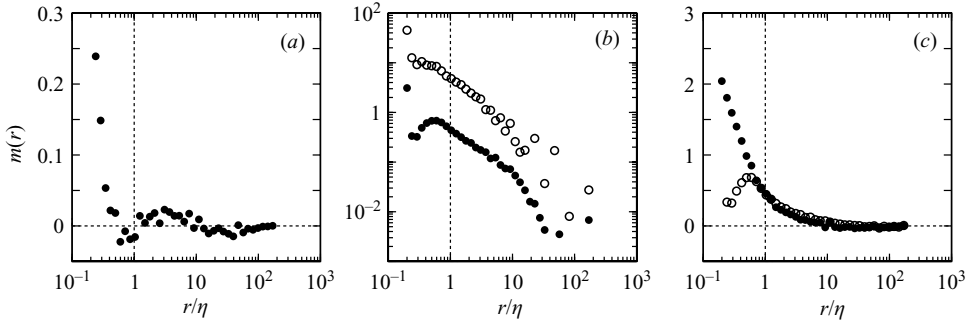
FIGURE 4. DNS pair correlation functions $m(r)$ of (*a*) inertial particles ($St = 0.4$), (*b*) zero-acceleration points (●) and zero-velocity points (○) and (*c*) inertial particles ($St = 1.9$, ●) and zero-acceleration points (○).

simulations we use this theorem and effectively calculate the right-hand side of (5) which is the clustering index divided by $\langle N \rangle_r$. This right-hand side is zero for Poisson spatial distributions. A power law $\overline{m}(r) \sim r^{-1}$ is an indication of a multiple size structure of near-empty regions except when $I = 1$, in which case the pair correlation function $m(r)$ is a constant different from zero up to a certain length scale (which characterizes the size of near-empty regions) and equal to 0 for r larger than this length scale. Increasing values of $\overline{m}(r)$ reflect increasing clustering.

For all intents and purposes the inertial particles' pair correlation function $m(r) \approx 0$ for $r \geqslant \eta$ and $m(r) \neq 0$ for $r < \eta$ in our DNS when $St < O(1)$ (see figure 4*a* where $m(r)$ is obtained from differentiation of $r\overline{m}(r)$ as in other such figures here). In figure 4(*b*) we plot the pair correlation functions $m(r)$ of zero-acceleration points and zero-velocity points (in the frame where the mean fluid flow is zero) obtained from our DNS. Zero-velocity points are more clustered than zero-acceleration points as the pair correlation functions (and therefore also $\overline{m}(r)$) of the zero-velocity points are larger by one order of magnitude than those of zero-acceleration points. Following the results of §4, we plot the pair correlation function of inertial particles for the case which corresponds with maximum values of $\overline{m}(r)$ for $r < \eta$ ($St = 1.9$) and find that it coincides quite closely with the pair correlation function of zero-acceleration points (see figure 4*c*). This result is in agreement with figure 2 where the remarkable spatial correlation between the spatial distributions of inertial particles and zero-acceleration points is shown directly.

6. Removing the large-scale sweeping of small scales

It is not possible to remove from the DNS turbulence the large-scale sweeping of small scales and the clustering of zero-acceleration points, so we now use a KS of two-dimensional homogeneous turbulence with a $-5/3$ power-law energy spectrum where the flow is synthesized in such a way that the sweeping and the acceleration clustering are absent by construction. The point of this exercise is to study turbulent clustering of inertial particles in the absence of such sweeping and clustering as the clustering of inertial particles seems to mirror that of zero-acceleration points via large-scale sweeping.

In our KS we use two-dimensional turbulent-like velocity fields (see FV for fuller details)

$$\boldsymbol{u} = \sum_{n=1}^{N_k} \boldsymbol{A}_n \cos(\boldsymbol{k}_n \cdot \boldsymbol{x} + \omega_n t) + \boldsymbol{B}_n \sin(\boldsymbol{k}_n \cdot \boldsymbol{x} + \omega_n t) \qquad (6)$$

where N_k is the number of modes, and the directions and orientations of $\boldsymbol{A}_n$ and $\boldsymbol{B}_n$ are chosen randomly and uncorrelated with the directions and orientations of all other wave modes but perpendicular to $\boldsymbol{k}_n$. The distribution of wavenumbers is geometric, specifically

$$k_n \equiv |\boldsymbol{k}_n| = k_1 \left(\frac{k_{N_k}}{k_1} \right)^{\frac{n-1}{N_k-1}}.$$

The velocity field is incompressible by construction, and also statistically stationary, homogeneous and isotropic as shown by FV and references therein. The amplitudes of the vectors $\boldsymbol{A}_n$ and $\boldsymbol{B}_n$ are determined from the energy spectrum $E(k_n)$ prescribed to be of the form

$$E(k) = \frac{u'^2}{(L/2\pi)^{2/3}} k^{-5/3} \qquad (7)$$

in the range $2\pi/L = k_1 \leqslant k \leqslant k_{N_k} = 2\pi/\eta$, and $E(k) = 0$ otherwise. Following FV, Osborne, Vassilicos & Haigh (2005) and Osborne *et al.* (2006), we set $\omega_n = \lambda \sqrt{k_n^3 E(k_n)}$, and test the dependence of our results on the dimensionless parameter λ (which controls the degree of unsteadiness of the turbulent-like flow) and on L/η.

Note that time scales which take some account of the large-scale sweeping correspond to frequencies $u' k_n$ rather than $\omega_n = \lambda \sqrt{k_n^3 E(k_n)}$ which do not (see Osborne *et al.* 2005). Also, there are no dynamics in KS, and in particular no provision for large-scale Fourier modes to advect small-scale ones. The idea behind KS is to synthesize a velocity field which can be thought of as an approximate ultimate result representative of some of the would-be turbulence dynamics in that it is incompressible, unsteady and incorporates some realistic statistics such as energy spectra. Even without any realistic representation of large-scale sweeping, KS contains enough information to produce good statistics of single and pairs of fluid elements (see Osborne *et al.* 2005, 2006 and references therein). Without large-scale sweeping, however, the arguments of §4 would suggest that KS cannot reproduce clustering of inertial particles.

First, we confirm that the sweeping is indeed absent in KS because the scaling (4) does not hold. What seems to hold instead is $V'_a/u' \sim (L/\eta)^{-1/3}$ (see figure 3b). This scaling is the same as that found by Goto *et al.* (2005) for V'_s, the r.m.s. of the velocities $\boldsymbol{V}_s$ of velocity stagnation points, and suggests that zero-acceleration points tend to move increasingly slowly relative to large-scale motions as L/η increases.

Secondly, we find that KS zero-acceleration points are uniformly distributed in space for all the values of λ ($\lambda = 0, 0.5, 5$) and L/η that we tried. This is confirmed by the pair correlation function $m(r)$ of zero-acceleration points which is found to be close to zero for all values of r between η and L (see figure 5a).

Surprisingly, however, inertial-particle position fields starting from initial uniformity do nevertheless develop well-defined near-empty spaces as time progresses, and furthermore, as with our DNS results, the locations of these near-empty spaces at given integration times (long enough compared to τ_p) are the same for all Stokes numbers tried (see figure 6) but their average size increases with increasing Stokes number (see Chen, Vassilicos & Fung 2006 for quantitative details and also Falkovich
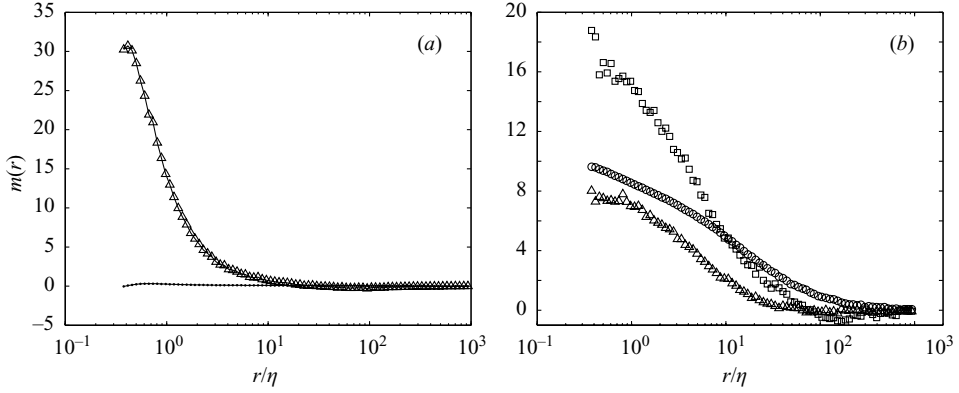
FIGURE 5. Two-dimensional KS, $L/\eta = 1000$. (*a*) $m(r)$ for zero-acceleration points ($\cdot$) and for zero-velocity points ($\triangle$); $\lambda = 0.5$. (*b*) $m(r)$ of inertial particles with $St = 1.6$. $\square$, $\lambda = 0$; $\bigcirc$, $\lambda = 0.5$; $\triangle$, $\lambda = 5.0$.
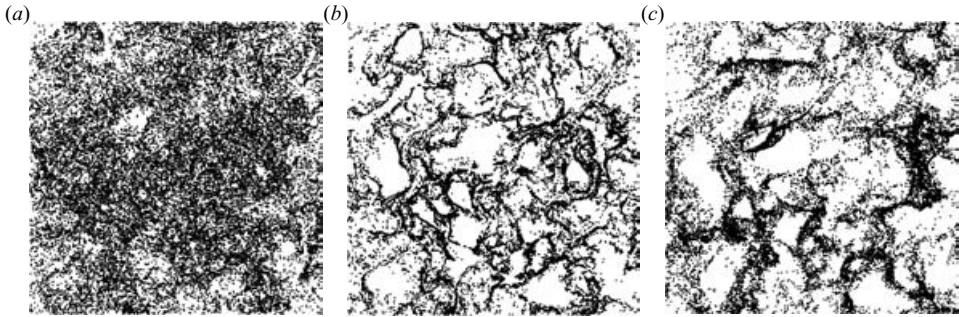

FIGURE 6. Particle distributions in two-dimensional KS turbulent-like velocity field. $L/\eta = 1000$, $\lambda = 0.5$. Box size is $2L$. (*a*) $St = 0.1$; (*b*) $St = 0.8$; (*c*) $St = 6.4$.

et al. 2003). This clustering occurs for values of λ that are small enough; for large values of λ (significantly larger than 5) clustering does not occur and the inertial particles remain uniformly distributed. These visual results are confirmed by the pair correlation function $m(r)$ of inertial particles which takes largest values for $\lambda = 0$, much smaller albeit significantly non-zero values for $\lambda = 0.5$ and values even smaller for $\lambda = 5$ (see figure 5*b*).

In our KS we find that as L/η increases, $\langle |\boldsymbol{\omega}|^2 \rangle_p / \langle |\mathbf{s}|^2 \rangle_p$ tends from below towards 2 with a rate of convergence which is faster for larger values of λ. As with our DNS results, the generation of near-empty spaces once again cannot be fully understood in terms of inertial particles escaping high-vorticity regions because near-empty spaces appear at as high values of L/η as we have tried when λ is not too large.

7. Persistent velocity stagnation points

So what causes clustering of inertial particles in KS? In figure 7 we plot velocity stagnation points (zero velocity in the frame where the mean flow is zero) and inertial particles at a time chosen long enough compared to τ_p. This figure comprises two plots, one for $\lambda = 0.5$ and one for $\lambda = 0$ (Chen *et al.* 2006 show that zero-acceleration points where the velocity is not zero exist in two-dimensional KS when $\lambda = 0$ and the velocity field is frozen; they are inflection points on streamlines where a velocity

extremum also occurs). In both cases, it is striking how inertial particles cluster in such a way as to avoid velocity stagnation points. One might say that inertial particles and velocity stagnation points anti-cluster. The clustering of velocity stagnation points is confirmed by their significantly non-zero values of $m(r)$ (see figure 5a) irrespective of the value of λ. Figure 8 shows two plots of inertial particles superimposed on the magnitudes of streamfunction, contours of which are streamlines. It is clear that inertial particles congregate where the average streamline curvature seems to be characteristically small and keep away from regions where the average streamline curvature is characteristically large. Streamline curvature is indeed largest in the vicinity of velocity stagnation points, and it may therefore not be too surprising to find that velocity stagnation points cluster where streamline curvature is relatively large. The behaviour observed in figures 7 and 8 is consistent with inertial particles being centrifugally flung out of regions of high streamline curvature near velocity stagnation points. This mechanism is reminiscent of the one proposed by Maxey & Corrsin (1986) and Maxey (1987) to explain the effects that turbulence can have on particle settling velocities. It requires the stagnation points to be persistent enough, which they are for small enough λ because, in this limit, they move slowly compared to u' (see Goto *et al.* 2005 and Osborne *et al.* 2006; in KS $V'_s/u' \sim \lambda$) and because they last long (see Osborne *et al.* 2006 who present an argument showing that the average life-time of velocity stagnation points scales with the integral time scale). Indeed, no particle clustering is observed when λ is large enough for a given value of L/η.

We would expect the centrifugal effect of highly curved streamlines around velocity stagnation points to exist in real high-Reynolds-number turbulence as it does in KS, in particular because these stagnation points are increasingly persistent with increasing Reynolds number as demonstrated by Goto *et al.* (2005) and Osborne *et al.* (2006). However, our DNS results do not reveal a clear imprint of this effect on particle clustering. Instead, our DNS results strongly suggest that inertial-particle clustering reflects the clustering of acceleration stagnation points.

GV have shown that the number density of zero-acceleration points scales as $(L/\eta)^d$ ($d = 2, 3$ for two and three dimensions respectively) whereas the number density of zero-velocity points (irrespective of frame of reference) scales as $(L/\eta)^{D_s}$ where $p + 2D_s/d = 3$ and p is the exponent of the power-law energy spectrum (see also Davila & Vassilicos 2003). There are therefore many more zero-acceleration points than zero-velocity points and Goto *et al.* (2005) have argued that, typically, zero-velocity points in the frame of reference where the mean fluid flow vanishes tend to become slow-moving zero-acceleration points. The persistence of these points is partly reflected in that, as a consequence, $(\partial/\partial t)\boldsymbol{u} = 0$ at these points in that frame. The remaining zero-acceleration points are not zero-velocity points.

These remaining zero-acceleration points are by far more numerous than the other zero-acceleration points and than zero-velocity points. It is therefore natural to expect the effect of their clustering on inertial-particle clustering to dominate over any effect that the persistent zero-velocity points may have. Of course, this is not to say that persistent zero-velocity points may not have an effect on other aspects of inertial-particle dispersion such as turbulent diffusivities and settling velocities.

8. Conclusion

In high-Reynolds-number two-dimensional turbulence with $-5/3$ power-law energy spectrum, stagnation points appear in clusters. Their pair correlation functions (see
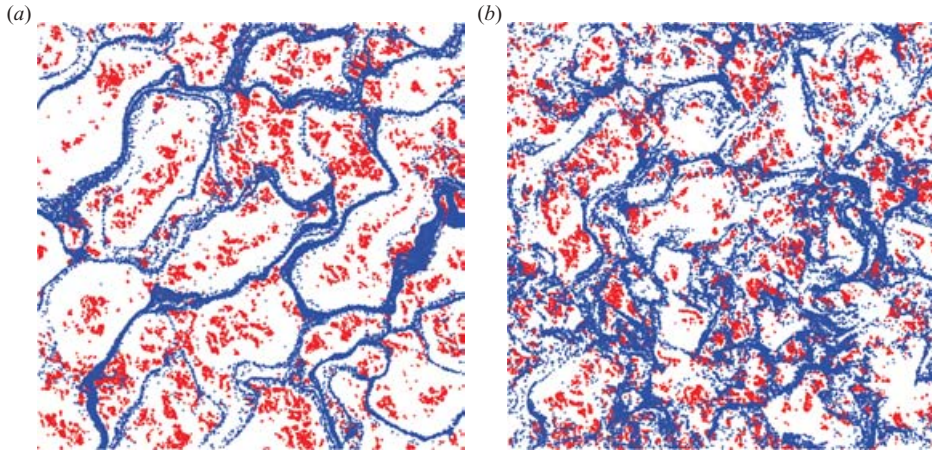
(*a*) (*b*)

FIGURE 7. Spatial distribution of inertial particles ($St = 1.6$) (in blue) and zero-velocity points (in red) in two-dimensional KS. $L/\eta = 1000$. Box size is $2L$. (*a*) $\lambda = 0$, (*b*) $\lambda = 0.5$.
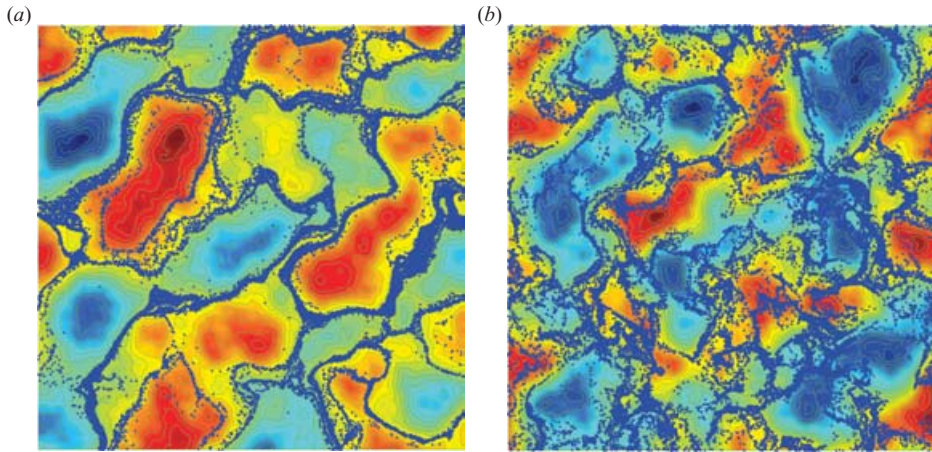
(*a*) (*b*)

FIGURE 8. Spatial distribution of inertial particles (blue dots) against a background of iso-streamfunction contours in two-dimensional KS. $L/\eta = 1000$. Box size is $2L$. (*a*) $\lambda = 0$, (*b*) $\lambda = 0.5$.

figure 4*b*) indicate that velocity stagnation points are more clustered than acceleration stagnation points.

Inertial particles in such turbulence also cluster, and their clustering reflects that of acceleration stagnation points for all Stokes numbers smaller than T/τ_η. Acceleration stagnation points and small inertial particles are swept by large-scale motions in such a way that inertial particles move away from points of non-zero acceleration towards acceleration stagnation points. In KS where large-scale sweeping is absent and where acceleration points do not cluster, inertial particles do nevertheless cluster as a result of the repelling action of velocity stagnation-point clusters. This repelling action has a negligible effect on inertial-particle clustering in high-Reynolds-number two-dimensional DNS turbulence.

It will be important to carry out studies with non-zero gravity for mixtures of different Stokes number particles (see Ghosh *et al.* 2005), and to take into account, in such studies, the fact that most eddies/vortices in turbulence are not isolated

but clustered. Indeed, the fact that eddies/vortices are clustered is rarely taken into account in studies of enhanced coalescence and precipitation, see for example Ghosh *et al.* (2005). Vaillancourt & Yau (2000) caution against droplet clustering mechanisms for explaining droplet spectral broadening in warm clouds because the Stokes numbers of cloud droplets are usually too small for them to be flung out of individual vortices and because the resulting concentration fluctuations may not be persistent enough in time. This caution ignores the findings of our present paper, i.e. that inertial particles can cluster as a result of the clustering of zero-acceleration points even when their Stokes number is small (see figure 1*a*, *b*), and that the large scales sweep zero-acceleration points and inertial particles together thus implying the kind of persistence in time which might well cause droplet spectral broadening to occur as a result of clustering.

REFERENCES

BOFFETTA, G., DE LILLO, F. & GAMBA, A. 2004 Large scale inhomogeneity of inertial particles in turbulent flows. *Phys. Fluids* **16**, L20.

CHEN, L., VASSILICOS, J. C. & FUNG, J. C. H. 2006 Clustering of inertial particles in the absence of large-scale sweeping (in preparation).

COLLINS, L. R. & KESWANI, A. 2004 Reynolds number scaling of particle clustering in turbulent aerosols. *New J. Phys.* **6**, 119.

DAVILA, J. & VASSILICOS, J. C. 2003 Richardson's pair diffusion and the stagnation point structure of turbulence. *Phys. Rev. Lett.* **91**, 144501.

FALKOVICH, G., FOUXON, A. & STEPANOV, M. 2003 Statistics of turbulence-induced fluctuations of particle concentration. In *Sedimentation and Sediment Transport* (ed. A. Gyr & W. Kinzelbach), p. 158 Kluwer.

FALKOVICH, G. & PUMIR, A. 2004 Intermittent distribution of heavy particles in a turbulent flow. *Phys. Fluids* **16**, L47.

FUNG, J. C. H. & VASSILICOS, J. C. 1998 Two-particle dispersion in turbulent-like flows. *Phys. Rev.* E **57**, 1677.

GHOSH, S., DAVILA, J., HUNT, J. C. R., SRDIC, A., FERNANDO, H. J. S. & JONAS, P. R. 2005 How turbulence enhances coalescence of settling particles with applications to rain in clouds. *Proc. R. Soc. Lond.* A **461**, 3059.

GOTO, S., OSBORNE, D. R., VASSILICOS, J. C. & HAIGH, J. D. 2005 Acceleration statistics as measures of statistical persistence of streamlines in isotropic turbulence. *Phys. Rev.* E **71**, 015301.

GOTO, S. & VASSILICOS, J. C. 2004 Particle pair diffusion and persistent streamline topology in two-dimensional turbulence. *New J. Phys.* **6**, 65.

GOTO, S. & VASSILICOS, J. C. 2006 Self-similar clustering of inertial particles and zero-acceleration points in two-dimensional turbulence (in preparation).

KOSTINSKI, A. B. & JAMESON, A. R. 2000 On the spatial distribution of cloud particles. *J. Atmos. Sci.* **57**, 901.

KOSTINSKI, A. B. & SHAW, R. A. 2001 Scale-dependent droplet clustering in turbulent clouds. *J. Fluid Mech.* **434**, 389.

LANDAU, L. D. & LIFSHITZ, E. M. 1980 *Statistical Physics*. Pergamon.

MAXEY, M. R. 1987 The gravitational settling of aerosol particles in homogeneous turbulence and random flow fields. *J. Fluid Mech.* **174**, 441.

MAXEY, M. R. & CORRSIN, S. 1986 Gravitational settling of aerosol particles in randomly oriented cellular flow fields. *J. Atmos. Sci.* **43**, 1112.

Maxey, M. R. & Riley, J. J. 1983 Equation of motion for a small rigid sphere in a nonuniform flow. *Phys. Fluids* **26**, 883.

Osborne, D. R., Vassilicos, J. C. & Haigh, J. D. 2005 One particle two-time diffusion in 3D homogeneous isotropic turbulence. *Phys. Fluids* **17**, 035104.

Osborne, D. R., Vassilicos, J. C., Sung, K. S. & Haigh, J. D. 2006 Fundamentals of pair diffusion in kinematic simulations of turbulence. *Phys. Rev.* E (submitted).

Shaw, R. A., Kostinski, A. B. & Larsen, M. L. 2002 Towards quantifying droplet clustering in clouds. *Qu. J. R. Met. Soc.* **128**, 1043.

Sundaram, S. & Collins, L. R. 1997 Collision statistics in an isotropic particle-laden turbulent suspension. *J. Fluid Mech.* **335**, 75.

Tennekes, H. 1975 Eulerian and Lagrangian time microscales in isotropic turbulence. *J. Fluid Mech.* **67**, 561.

Vaillancourt, P. A. & Yau, M. K. 2000 Review of particle-turbulence interactions and consequences for cloud physics. *Bull. Amr. Met. Soc.* **81**, 285.